

Soliton electro-optic effects in paraelectrics

Eugenio DelRe and Mario Tamburrini

Fondazione Ugo Bordoni, Via B. Castiglione 59, 00142 Roma, Italy, and INFN, Unita' di Roma I, Italy

Aharon J. Agranat

Applied Physics Department, Hebrew University of Jerusalem, Jerusalem 91904, Israel

(October 29, 2018)

The combination of charge separation induced by the formation of a single photorefractive screening soliton and an applied external bias field in a paraelectric is shown to lead to a family of useful electro-optic guiding patterns and properties.

Apart from their inherent interest as peculiar products of nonlinearity, spatial solitons hold the promise of allowing viable optical steering in bulk environments [1] [2]. Photorefractive screening solitons differ from other known manifestations of spatial self-trapping for their peculiar ease of observation and versatility [3], and recent experiments in photorefractive strontium-barium-niobate (SBN) and potassium-niobate (KNbO_3) have demonstrated two conceptual applications of their guiding properties. In the first case, a tunable directional coupler was realized making use of two independent slab-solitons [4]; in the second, self-induced phase-matching was observed to enhance second-harmonic-generation [5]. Although results suggest a means of obtaining all-optical functionality, actual implementation is hampered by the generally slow nonlinear response [6], that can be "accelerated" only at the expense of stringent intensity requirements [7]. In contrast, non-dynamic guiding structures have been observed by fixing a screening soliton [8], or in relation to the observation of spontaneous self-trapping during a structural crystal phase-transition [9]. One possible method of obtaining acceptable dynamics is to make directly use of the electro-optic properties of the ferroelectrics involved, in combination with the internal photorefractive space charge field deposited by the soliton. Since photorefractive charge-activation is wavelength dependent, one can induce charge separation in soliton-like structures at one active wavelength (typically visible), and then read the electro-optic index modulation at a different, nonphotorefractive, wavelength (typically infrared) [10] [11]. For *non-centrosymmetric* samples (such as the above mentioned crystals) that typically host screening soliton formation, the electro-optic index of refraction modulation is proportional to the static crystal polarization \mathbf{P} , and thus to the electric field (linear electro-optic effect). For these, *no* electro-optic modulation effects are possible: for whatever value of external constant electric field E_{ext} , the original soliton supporting guiding pattern remains *unchanged*. In *centrosymmetric*s, such as photorefractive potassium-lithium-tantalate-niobate (KLTN), soli-

tons are supported by the quadratic electro-optic effect [12] [13] [14] [15]. In this case, the "nonlinear" combination of the internal photorefractive field with an external electric field can give rise to new and useful soliton-based electro-optic phenomena, which we here study for the first time.

The basic mechanism leading to screening soliton formation is the following: a highly diffracting optical beam ionizes impurities hosted in the lattice of an electro-optic crystal. An externally applied electric field makes these mobile charges drift to less illuminated regions, forming a double layer that renders the resultant electric field in the illuminated region lower. For an appropriate electro-optic sample, this leads to a self-lensing and soliton propagation, when beam diffraction is exactly compensated. For slab solitons, i.e. those self-trapped beams that originate from a beam that linearly diffracts only in one transverse dimension (x), for a given soliton intensity full-width-half-maximum (FWHM) Δx , a given ratio between the soliton peak intensity and the (generally artificial) background illumination, $u_0^2 = I_{peak}/I_b$ (intensity ratio), solitons form for a particular value of applied external biasing field \bar{E} . The soliton-supporting electric field E is expressed by $E=(V/L)(1+I(x)/I_b)^{-1}$, where V is the external applied voltage, L is the distance between the crystal electrodes (thus $\bar{E}=V/L$), and $I(x)$ is the soliton optical intensity confined in the x transverse dimension [12]. This electric field, a result of a complex nonlinear light-matter interaction, is present even when the generating optical field is blocked, and the sample is illuminated with a nonphotorefractively active light. Charge separation is smeared out only by slow recombination, associated with dark conductivity, characterized by considerably long decay times. The nonphotorefractively active illumination, although not leading to any further evolution in the internal charge field, will feel the index inhomogeneity due to the quadratic electro-optic response described by the relation $\Delta n = -(1/2) n^3 g_{eff} \epsilon_0^2 (\epsilon_r - 1)^2 E^2$, where n is the crystal index of refraction, g_{eff} is the effective electro-optic coefficient for a given scalar configuration, ϵ_0 is the vacuum dielectric constant, and ϵ_r is the

relative dielectric constant. The actual electric field in the crystal is now $E=(V/L)(1+I(x)/I_b)^{-1}-(V/L)+E_{ext}$, where E_{ext} (in general $\neq \bar{E}$) is the externally applied electric field *after* the nonlinear processes have occurred (the "read-out" field). The index pattern induced is

$$\Delta n = -\Delta n_0 \left(\frac{1}{1 + I(x)/I_b} - 1 + \frac{E_{ext}}{V/L} \right)^2, \quad (1)$$

where $\Delta n_0 = (1/2) n^3 g_{eff} \epsilon_0^2 (\epsilon_r - 1)^2 (V/L)^2$. In Fig.(1) we show two families of induced index patterns associated with two solitons at different saturation levels. In Fig.(1a) a $7\mu\text{m}$ FWHM soliton at $\lambda=514\text{ nm}$ wavelength ($\Delta n_0 \simeq 5.4 \times 10^{-4}$, for $n=2.45$) with an intensity ratio $u_0^2=4$, leads to three characteristic pattern regimes: for $\eta = E_{ext}/(V/L) \simeq 1$, the soliton supporting potential is formed. For $\eta \simeq 0$, an antiguiding hump appears, whereas for intermediate values of η , a twin-waveguide potential forms. Analogous results can be predicted for a strongly saturated regime shown in Fig.(1b), where a $11\mu\text{m}$ soliton is formed for $u_0^2 \simeq 22$.

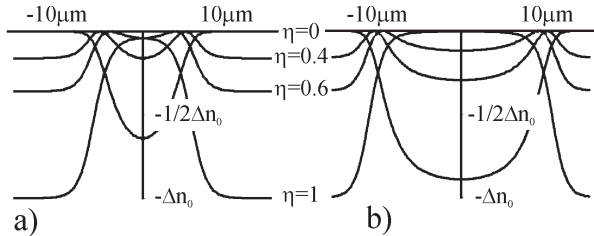


FIG. 1. Predicted electro-optic index patterns resulting from the soliton deposited space-charge field, for $u_0 = 2$ (a) and $u_0 = 4.7$ (b).

Experiments are carried out with an apparatus that is well documented in literature [13] [14]. An enlarged TEM₀₀ Gaussian beam from a CW Argon-ion laser operating at $\lambda = 514\text{nm}$, is focused by means of an $f=150\text{mm}$ cylindrical lens onto the input facet of an $3.7^{(x)} \times 4.6^{(y)} \times 2.4^{(z)}$ mm sample of zero-cut paraelectric KLTN, at $T=20^\circ\text{C}$ (with a critical temperature $T_c=11^\circ\text{C}$), giving rise to an approximately one-dimensional x-polarized Gaussian beam of $\Delta x \simeq 11\mu\text{m}$ ("soliton" beam), and the entire crystal is illuminated with a second, homogeneous beam ("background" beam) from the same laser, polarized along the y axis. Both the focused and the plane-wave beams copropagate along the z-direction. The constant voltage V is applied along the crystal x direction, the crystal itself being doped with Vanadium and Copper impurities, and photorefractively active at the laser wavelength. Guiding patterns can be investigated either by illuminating the crystal with an infrared beam (as mentioned above), or simply by using the same soliton-forming wavelength, but at a lower intensity, since photorefractive temporal dynamics are proportional to beam intensity. Here we use this read-out method, and in

what follows all read/write experiments are at $\lambda=514\text{nm}$, with $I_{read}/I_{write} \simeq 20$. By changing the value of the applied readout voltage, V_{ext} , we can explore the optical potential described by Eq.(1), through the variable η . Beam distribution is investigated by imaging the facets of the sample onto a CCD camera by means of a second lens placed after the sample (along the z direction).

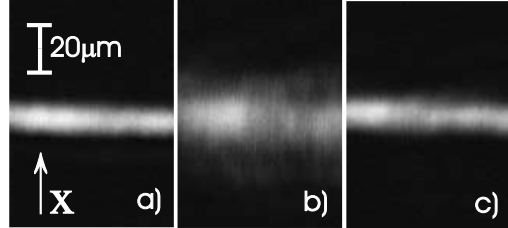


FIG. 2. Soliton formation: an input $11\mu\text{m}$ beam (a) diffracts to $24\mu\text{m}$ in linear propagation ($V=0$) (b) and self-traps for $V_{exp}=1.33\text{ kV}$ at $T=20^\circ\text{C}$, for $u_0 \simeq 4.7$.

In Fig.(2) the observation of a single photorefractive screening soliton is shown. The $11\mu\text{m}$ soliton is observed with an intensity ratio $u_0^2 \simeq 22$ at $V_{exp}=1.33\text{ kV}$, annulling linear diffraction to $24\mu\text{m}$. Soliton formation takes approximately 3 min, for an $I_{peak} \simeq 1.8\text{ kW/m}^2$ ($I_b \simeq 80\text{ W/m}^2$), measured directly before the sample, thus meaning that erasure during readout would take, at the very least, about 1 hr (i.e. longer than the duration of any one of our experiments). Had we used an IR read-out beam, decay would be halted indefinitely. Given the sample $g_{eff}=0.12\text{m}^4\text{C}^{-2}$, $\epsilon_r \simeq 9000$, $\Delta n_0 \simeq 6.9 \times 10^{-4}$, the expected value for soliton formation would be $V_{th} \simeq 1.27\text{ kV}$.

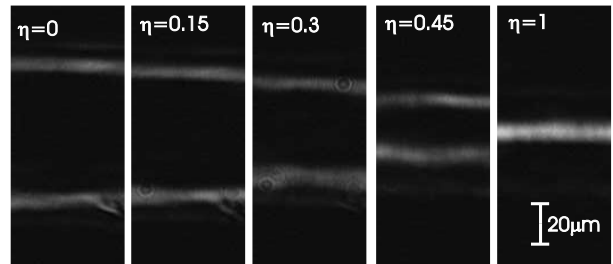


FIG. 3. Output light distribution of the read-out beam. For $\eta=0-0.3$ the beam is scattered. For $\eta=0.45$ the twin beam structure forms, whereas for $\eta=1$ the original guiding pattern emerges.

In Fig.(3) we show the same region of the crystal investigated by the less intense (but otherwise identical to the soliton generating) "read" beam at various values of η . For $\eta=1$ the output beam is identical to the soliton (apart

from the actual intensity). For low values of η ($\eta < 0.4$) the index pattern given by Eq.(1) is antiguiding, and the output beam is scattered and split into two diffracting beams (beam "bursting", see Fig.(1b)). As η is increased, the defocusing is weakened and for $\eta \approx 0.45$ the sample gives rise to a beam-splitting on the twin-waveguide structure formed by the two-hump potential, as shown in Fig.(1). The distance between the two beams is $\approx 20\mu\text{m}$. As opposed to previous defocusing, in this case light is exciting a guided mode.

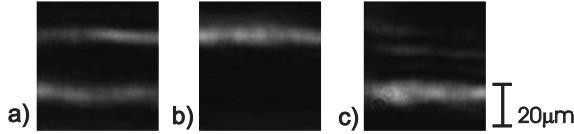


FIG. 4. Electro-optic switching. The output light distribution of the read beam (a) for $\eta=0.45$, the side-guided beam, when the crystal is shifted sideways of $10\mu\text{m}$ (b), the output in the same condition, but with $\eta=0.8$ (c).

Next we shift the crystal with respect to the optical beam in the x direction, so as to launch it directly into one of the twin-guides for intermediate values of η . For an $\eta=0.45$, shifting the crystal by $10\mu\text{m}$, the beam is guided by the side hump, as shown in Fig.(4b). In this forward guiding condition, we change η to $\eta=0.8$. The potential commutes from a double-hump twin-waveguide to a single guiding pattern (see Fig.1). The optical beam is redirected as shown in Fig.(4c).

It is therefore possible to realize, by means of the formation of a single photorefractive centrosymmetric screening soliton, three qualitatively different optical circuits: a single waveguide, a double waveguide beam-splitter, and an antiguiding beam-stopper. If the crystal is shifted so as to launch the guided beam into one of the twin-guides, it is possible to deviate the beam, maintaining its strong confinement, realizing an electro-optic switch. Had we used a longer sample, launching the beam in a twin-waveguide leads to a tunable directional coupler, as shown in Fig.(5).

The observed phenomena represent an important step in the achievement of viable soliton based components in two major aspects. The first is that the observed phenomenology occurs with the formation of a single soliton, that is only used to deposit a pattern of charge displacement (a peculiar volume hologram), whereas switching from one regime to the other occurs only through the change of the applied electric field. Thus switching dynamics are only limited by capacity charging times, as all other electro-optic devices. Secondly, whereas screening soliton *formation* requires a constant applied external field, during read-out, the use of independent electrodes can allow the formation of composite circuitry in cascade, all from a single soliton.

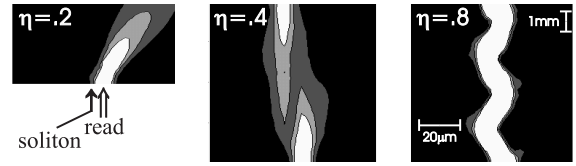


FIG. 5. Predicted evolution of an $\approx 7\mu\text{m}$ beam: top view of read-out in an 8mm sample for $\eta=0.2$ (beam deflection and diffraction) (left), one beat directional coupling for $\eta=0.4$ from right hump to left hump (center), and mode beating for $\eta=0.8$ ($\approx 2\text{mm}$ mode beat).

The work of E.D. and M.T. was carried out in the framework of an agreement between Fondazione Ugo Bordoni and the Italian Communications Administration. Research carried out by A.J.A. is supported by a grant from the Ministry of Science of the State of Israel.

-
- [1] G.I. Stegeman and M. Segev, *Science* **286**, 1518 (1999).
 - [2] M. Segev and M. Stegeman, *Phys. Today* **51**, 42 (1998).
 - [3] B. Crosignani, P. Di Porto, M. Segev, G. Salamo, and A. Yariv, *Riv. Nuovo Cimento* **21**, 1 (6) (1998).
 - [4] S. Lan, E. DelRe, Z. Chen, M. Shih, and M. Segev, *Opt. Lett.* **24**, 475 (1999).
 - [5] S. Lan, M. Shih, G. Mizell, J. A. Giordmaine, Z. Chen, C. Anastassiou, J. Martin, and M. Segev, *Opt. Lett.* **24**, 1145 (1999).
 - [6] L. Solymar, D. J. Webb, and A. Grunnet-Jepsen, *The physics and applications of photorefractive materials* (Clarendon Press, Oxford 1996).
 - [7] K. Kos, G. Salamo, and M. Segev, *Opt. Lett.* **23**, 1001 (1998).
 - [8] M. Klotz, H. Meng, G. J. Salamo, M. Segev, and S. R. Montgomery, *Opt. Lett.* **24**, 77 (1999).
 - [9] E. DelRe, M. Tamburrini, M. Segev, R. Della Pergola, and A. J. Agranat, *Phys. Rev. Lett.* **83**, 1954 (1999).
 - [10] M. Shih, Z. Chen, M. Mitchell, M. Segev, H. Lee, R. S. Feigelson, and J. P. Wilde, *J. Opt. Soc. Am. B* **14**, 3091 (1997).
 - [11] For linear schemes based on screening see A. Bekker, A. Ped'el, N. K. Berger, M. Horowitz, and B. Fisher, *Appl. Phys. Lett.* **72**, 3121 (1998) and Ph. Dittrich, G. Montemezzani, P. Bernasconi, and P. Gunter, *Opt. Lett.* **24**, 1508 (1999).
 - [12] M. Segev and A. J. Agranat, *Opt. Lett.* **22**, 1299 (1997).
 - [13] E. DelRe, B. Crosignani, M. Tamburrini, M. Segev, M. Mitchell, E. Refaeli, and A. J. Agranat, *Opt. Lett.* **23**, 421 (1998).
 - [14] E. DelRe, M. Tamburrini, M. Segev, E. Refaeli, and A. J. Agranat, *Appl. Phys. Lett.* **73**, 16 (1998).
 - [15] A.J. Agranat, R. Hofmeister, and A. Yariv, *Opt. Lett.* **17**, 713 (1992).